Applied Geochemistry 100 (2019) 258–267

Contents lists available at ScienceDirect

Applied Geochemistry

journal homepage: www.elsevier.com/locate/apgeochem

Modeling of strontium leaching from carbonated Portland cement pastes using a simplified diffusion-kinetic analytical model

E. Boukobza[a,b,*,1], G. Bar-Nes[a], O. Klein Ben-David[a,c], B. Carmeli[a,1]

[a] Chemistry Department, Nuclear Research Center Negev, 84190, Israel
[b] School of Chemistry, Tel-Aviv University, Tel-Aviv, 6997801, Israel
[c] Dep. of Geology and Environmental Sciences, Ben Gurion University of the Negev, Be'er Sheva, 8410501, Israel

ARTICLE INFO

Editorial handling by Prof. M. Kersten

Keywords:
Leaching
Cement
Modeling
Carbonation

ABSTRACT

One of the main challenges in nuclear waste management is to predict release of radionuclides during their long-term disposal within an intact matrix in the repository. One way to tackle this challenge is to conduct leaching experiments which emulate radionuclide release under extreme conditions in a relatively short time. In this work we present a simple analytical diffusion-kinetic model for strontium leaching from cylindrical samples of Portland cement paste. The model accounts explicitly for both strontium diffusion and strontium carbonate precipitation. We compare this model with a standard diffusion model, and demonstrate that it better fits experimental strontium leaching data from samples that showed minor carbonation, as well as samples that showed atmospheric carbonation. This diffusion-kinetic model gives rise to narrower prediction bounds and substantially smaller errors. Furthermore, it provides experimentalists conducting leaching tests an easily implementable tool to analyze their data in systems where precipitation is expected to occur. The approach presented here may serve as an alternative to a plain diffusion analysis often found in standardized leaching protocols, and to more intricate thermodynamic numerical software.

1. Introduction

Radioactive waste management is a serious endeavor to modern societies, with grave implications for future generations. In this vast and rapidly growing field, radionuclide release experiments of hazardous materials from engineered matrices and natural geological barriers are an important tool for assessing the dispersion of contaminants into the environment. These small scale, short term experiments, either emulate thermodynamic liquid-solid partitioning of buried waste under high liquid to solid ratio (e.g. 10 ml of water to 1 g solid matrix) and under full exposure of the matrix to the liquid (by grinding the matrix), or simulate accelerated radionuclide kinetic release conditions. Therefore, radionuclide release experiments can be divided into two categories. The first group of liquid/solid partitioning experiments are targeted to give an estimation on the partitioning of a given element/compound under equilibrium conditions, and hence are suitable for an intermediate-long time range prediction (e.g. EPA methods 1313 and 1314 in the US (Method 1313, 2012; Method 1314, 2013); CEN/TS 14429; CEN/TS 14997 and CEN/TS 14405 in the EU (CEN/TS 14429, 2005; CEN/TS 14405, 2004)). The second group of experiments are targeted to give the temporal release behavior for a given material under laboratory-controlled accelerated conditions (e.g. Methods 1315 and ANSI/ANS 16.1 in the US (Method 1315, 2013; ANSI/ANS 16.1, 2017); CEN/TS 15863 in the EU (CEN/TS 15863, 2009)).

In this study we present a simple analytical 3D (with axial symmetry) chemical transport (diffusion-kinetic) model for strontium leaching from a finite cylinder composed of Portland cement paste. The model is intended to give a macroscopic description for both strontium diffusion and strontium carbonate precipitation (due to atmospheric carbonation) for a set of leaching experiments previously presented by Bar-Nes et al. (Bar-Nes et al., 2018).

In the scientific literature, leaching is modeled by several different approaches. These can be divided into two main categories: kinetic and thermodynamic, both rely on the diffusion equation. The work by Abdel Rahman and Zaki (Abdel Rahman and Zaki, 2011) is an example of a comparative study of several conceptual generic kinetic models. In (Abdel Rahman and Zaki, 2011), explicit algebraic expressions for the cumulative leached fraction (CLF) are fitted to data sets. These expressions are empirical, and are *not* derived from chemical transport

* Corresponding author. School of Chemistry, Tel-Aviv University, Tel-Aviv, 6997801, Israel.
E-mail address: erezbou@gmail.com (E. Boukobza).
[1] Equal contribution.

https://doi.org/10.1016/j.apgeochem.2018.11.014
Received 14 June 2018; Received in revised form 30 October 2018; Accepted 19 November 2018
Available online 20 November 2018
0883-2927/

equations with underlying equilibrium reactions or reaction mechanisms. They may represent a first order kinetic rate law for a reaction in an outer layer of the matrix, a short temporal square root law for diffusion, linear dissolution process, or a combination of some/all the above-mentioned processes. We note that combining various physical and chemical processes involved in leaching experiments, does not necessarily yield a simple mathematical addition/multiplication of the individual expressions describing each process when deriving an overall expression for the CLF, as can be inferred from some of the expressions in (Abdel Rahman and Zaki, 2011). Therefore, combining diffusion with reaction kinetics requires close derivation for all time scales. This is provided in this work for strontium leaching on a short-intermediate time scale of up to three months.

Geochemical modeling software combining diffusion with local thermodynamic equilibrium calculations can be divided into two main categories: the law of mass action (LMA) and free energy minimization (FEM).

The foundations for LMA calculations in multiphase/multicomponent systems relying on knowledge of reaction equilibrium and partition constants were laid in the pioneering work of Brinkley, 1946, 1947. These principles were essentially implemented in the work of Morel and Morgan (1972) for concentrations in the liquid phase and calculation of salt saturation indices. More recent implementations of these principles are found in software such as PHREEQC (Parkhurst, 1995) and LeachXS (Kosson et al., 2014) for both the aqueous and solid phases. These software rely on the notion of *tenads*– chemical entities whose masses are reaction invariant, and in turn allow substantial simplifications of the reactive transport equations (Rubin, 1983).

The foundations of FEM calculations were laid in the pioneering work of White, Johnson and Dantzig (White et al., 1957). These were originally presented for the gas phase but are straightforwardly extendable for the liquid and solid phases. With the invention of the interior point method (IPM) by Dikin (1967), faster conversion is achieved in its implementation due to Karpov, Kulik and coworkers (Karpov et al., 1997, 2001) in geochemical software such as GEMS (Kulik et al., 2013).

Several examples of thermodynamic modeling of simple calcium silicate hydrate (CSH) mixtures as a function of Ca/Si ratio can be found in the literature, and are reviewed in (Soler, 2007). However, the fitting of measured analytical data of Ca and especially Si is not always perfect, and sometimes plotted on a logarithmic scale, hence differences between models and experiments can be substantial.

The main purpose of this work is to present an alternative kinetic approach to the thermodynamic modeling track, often found in the scientific literature when modeling either analytical compositions of cements, or leaching data. Our motivation is as follows. Since not always thermodynamic software can account for analytical Ca/Si data as major constituents in equilibrium liquid/solid partitioning tests, we cannot perfectly trust them to model minor constituents or materials added to cements, especially when they are involved in the chemistry of the major constituents, which includes transport. Therefore, our choice to kinetically model strontium leaching in carbonated cement pastes is natural, as both calcium and strontium tend to precipitate with the common carbonate anion. Moreover, since strontium is a common fission product in the nuclear industry its immobilization is of major importance in nuclear waste management, and hence serves as an additional motivation for this study.

The paper is arranged as follows. Section II is the heart of this work. In section II we describe the model, the governing equations, as well as their solution at short times. In addition, in Section II we give a probabilistic view of the CLF, and discuss the nature of the fitted diffusion coefficient. In section III we give a concise description of the leaching experiments, and compare the analytical solutions with the experimental data and fit global effective parameters for both the strontium diffusivity and the phenomenological first-order precipitation rate constant at short diffusion times. Section III also provides some sensitivity analysis of the analytical diffusion-kinetic CLF, and suggests criteria to rule out a simple diffusion scenario based on a simple linear graphical analysis. Section IV presents a discussion and conclusions of the present work, as well as perspective on future research.

2. Analytical model for strontium cumulative leached fraction (CLF)

2.1. Model description and kinetics of leaching

We describe a model in which Sr^{2+}ions diffuse inside a finite cement cylinder, and escape outside its external boundaries. The faces of the cylinder are treated as perfectly absorbing due to an occasional replacement of the surrounding aqueous solution, and hence represent Dirichlet boundary conditions of zero strontium concentration on its outer surfaces.

During diffusion, ions may be irreversibly trapped by carbonate ions embedded within the cement diffusive phase of the cement, and irreversibly precipitate. This description is a simplified relative to the true picture (in which various minerals are spread inside the cylindrical cement sample and mutually interact), mainly for two reasons. First, the diffusion inside the cement cylinder is in fact an averaged effective/apparent diffusion of Sr^{2+} ions in an aqueous solution within pores of the various cement phases. Second, the irreversible accumulation of strontium carbonate may occur as a dissolution-precipitation process within the various calcium carbonate phases. In such a process, precipitated calcium carbonate dissolves, and the carbonate ions re-precipitate with free Sr^{2+} ions.

We have three main assumptions in our model.

A) The diffusion coefficient of strontium is uniform in space. The simple analytical model presented here does not give a heterogeneous description of the cylindrical sample in which there are regions with a varying diffusion coefficient. Porosity is uniform as well.

B) Sr^{2+} ions are homogeneously distributed within the cement matrix prior leaching, which in turn boils down to the assumption that there is no substantial strontium concentration gradient during cement curing and incubation. This was not determined in the experiments, and although a strontium gradient might exist in the cement matrix prior leaching, it is expected to be significantly smaller than the concentration gradient during leaching (in which the concentration of strontium outside the cylinder is practically zero).

C) Strontium carbonate precipitation: $Sr^{2+}_{(aq)} + CO^{2-}_{3(aq)} \rightarrow SrCO_{3(s)}$; $K_{sp} \sim 5{\cdot}10^{-10}$, follows an irreversible pseudo first-order kinetics, with a homogeneous kinetic rate constant throughout the sample. The simple analytical model presented here does not give a heterogeneous description of the cylindrical sample in which there are regions where strontium precipitates and regions where no precipitation occurs. The assumption that strontium precipitation follows first-order kinetics is somewhat arbitrary. However, it is physically reasonable, as the total carbonate excess over strontium is 10–65-fold (for the samples discussed in (Bar-Nes et al., 2018) with minor and atmospheric carbonation, respectively), and allows a simple analytical solution for the overall strontium content at short times.

The three assumptions comprise a set of “mean-field" type assumptions, and represent an environment bridging minor and major precipitation regions in which diffusion-kinetic parameters assume an average value throughout the matrix. In essence, our approach can be viewed as a variant of a representative elementary volume approach, in which heterogeneity is averaged.

The equation describing the evolution of the concentration, $C\ [mg\ Sr/m^3\ cement]$, of the moving Sr^{2+} ions combines diffusion and a

first order precipitation rate.

$$\dot{C} = D_{ap}\nabla^2 C - kC \tag{1}$$

where D_{ap} is an apparent diffusion coefficient in the cement paste, and k is the apparent first order precipitation rate constant. Therefore, Eq. (1) reflects the two main processes involving strontium: diffusion and precipitation.

The evolution of the precipitated strontium mass, M, is given by:

$$\dot{M} = km \tag{2}$$

where m, the mass of the Sr^{2+} ions integrated over the volume of the cylinder is formally written as:

$$m = \int_{Cyl} dVC \tag{3}$$

We denote the initial free and precipitated Sr mass prior to the leaching step m_0 and M_0, respectively. By substitution, the formal solution of Eq. (1) is obtained by setting:

$$C(t, r, z) = F(t, r, z)e^{-kt} \tag{4}$$

where the function F solves the diffusion equation $\dot{F} = D\nabla^2 F$ with no sinks/sources.

By substituting Eq. (4) into Eq. (3) we trivially find:

$$m(t) = e^{-kt}\bar{m};\ \ \bar{m} = \int_{Cyl} dVF \tag{5}$$

The formal solution of Eq. (2) is hence:

$$M(t) = M_0 + k\int_0^t dt' e^{-kt'}\int_{Cyl} dVF \tag{6}$$

From these results the time evolution of the CLF, η, is readily obtained:

$$\eta = 1 - \frac{M(t) + m(t)}{M_0 + m_0} = \frac{1}{m_T^0}\left(m_0 - e^{-kt}\int_{Cyl} dVF - k\int_0^t dt' e^{-kt'}\int_{Cyl} dVF\right) \tag{7}$$

We note that although we do not know m_0 or M_0 prior leaching, we do know the total strontium content initially present in each sample, $m_T^0 = m_0 + M_0$, which is the sum of the spiked and intrinsic concentration (in mg Sr/g paste) multiplied by the sample's mass.

2.2. Diffusion from a finite cylinder and the CLF at short times

The uniform reactionless (no precipitation, $k = 0$) diffusion equation in axial-symmetric cylindrical coordinates is given by:

$$\frac{\partial F}{\partial t} = D\left[\frac{1}{r}\frac{\partial}{\partial r}\left(r\frac{\partial F}{\partial r}\right) + \frac{\partial^2 F}{\partial z^2}\right] \tag{8}$$

Where F is the concentration of free Sr^{2+} ions. The overall mass of free Sr^{2+} ions remaining in the cylinder due to diffusion only, $\overline{m(t)}$, for an initial uniform distribution, and zero concentration outside the cylinder is given by (Crank, 1975):

$$\overline{m(t)} = \int_{Cyl} dVF = m_0 U(t)W(t) \tag{9}$$

where

$$U(t) = \frac{8}{\pi^2}\sum_{n=0}^{\infty}\frac{1}{(2n+1)^2}e^{-(2n+1)^2\pi^2\frac{Dt}{H^2}} \tag{10a}$$

$$W(t) = 4\sum_{n=0}^{\infty}\frac{1}{\lambda_n^2}e^{-\lambda_n^2\frac{Dt}{R^2}} \tag{10b}$$

Using the Laplace transform method for short times (see also Appendix A):

$$\overline{m(t)} = \int_{Cyl} dVF = m_0\left(1 - \frac{4}{\sqrt{\pi}}\frac{\sqrt{Dt}}{L}\right) \tag{11}$$

where

$$\frac{1}{L} = \frac{1}{R} + \frac{1}{H} \tag{12}$$

Finally, by substituting the short time expansion for $\overline{m(t)}$ (Eq. (11)) into Eqs. (5) and (6) we obtain explicit short time expansions for free and precipitated strontium:

$$m(t) = m_0 e^{-kt}\left(1 - \frac{4}{\sqrt{\pi}}\frac{\sqrt{D_{ap}t}}{L}\right) \tag{13}$$

$$M(t) = M_0 + m_0\left[1 - e^{-kt}\left(1 - \frac{4}{\sqrt{\pi}}\frac{\sqrt{D_{ap}t}}{L}\right) - \frac{2\sqrt{D_{ap}}}{L}\frac{erf(\sqrt{kt})}{\sqrt{k}}\right] \tag{14}$$

The error function in Eq. (14) arises from a finite integral over a Gaussian through a change of the time variable in the integrand. When Eqs. (13) and (14) are substituted in Eq. (7), the CLF is finally obtained:

$$\eta = \nu\frac{2\sqrt{D_{ap}}}{L}\frac{erf(\sqrt{kt})}{\sqrt{k}} \tag{15}$$

where $\nu = m_0/m_T^0$ is the fraction of leachable strontium prior to the leaching step (after cement curing and sample incubation). Since we cannot separate ν from $\sqrt{D_{ap}}$ (single multiplicative factor), and no strontium carbonate measurement was carried out prior to leaching, we recast Eq. (13) as:

$$\eta = \frac{2\sqrt{\bar{D}_{ap}}}{L}\frac{erf(\sqrt{kt})}{\sqrt{k}} \tag{16}$$

where $\bar{D}_{ap} = \nu^2 D_{ap}$ is a scaled apparent diffusion coefficient.

In the limit $k \to 0$ ($M_0 = 0$), Eq. (13) converges to the standard diffusion result at short times:

$$\eta = 1 - \frac{m(t)}{m_0} = \frac{4\sqrt{D_e t}}{\sqrt{\pi}L} \tag{17}$$

where D_e is an effective diffusion coefficient.

2.3. General probabilistic view of the CLF

By substitution of Eq. (9) for free strontium due to diffusion only into Eq. (7) for the CLF, and integrating the latter by parts we obtain:

$$\eta = \nu\left(1 - e^{-kt}f(t) - k\int_0^t dt'\ e^{-kt'}f(t')\right) = \nu\int_0^t dt'\ e^{-kt'}\left(-\frac{df(t')}{dt'}\right) \tag{18}$$

where $f(t) = U(t)W(t)$.

Eq. (17) assumes the following interpretation: The probability to find a Sr^{2+} cation outside the cylinder, i.e. the CLF, is a product of the probability that initially the cylinder contains Sr^{2+} cations, ν, by the accumulated probability that these cations escape out of the cylinder. The latter probability is the accumulation (time integral) of the probability density to escape by the time t, which is by itself the product of probability that Sr^{2+} cations survived precipitation e^{-kt}, and the probability density to diffuse toward the boundary, $-\frac{df(t)}{dt}$.

2.4. The nature of the fitted diffusion coefficient

Several models exist in the scientific literature to model porous media through a representative elementary volume (REV) approach, for example (Ukrainczyk and Koenders, 2014; Seigneur et al., 2017; Bruna and Chapman, 2015; Valdés-Prada and Ramírez, 2011). In the work by

Bruna and Chapman the following diffusion-advection equation is presented after separating two coordinate scales:

$$\frac{\partial C(x)}{\partial t} = \vec{\nabla}_x \cdot \left[\psi(x) D_e(x) \vec{\nabla}_x \left(\frac{C(x)}{\psi(x)} \right) \right] = \vec{\nabla}_x \cdot \left[D_e(x) \vec{\nabla}_x C(x) - \frac{D_e(x) \vec{\nabla}_x \psi(x)}{\psi(x)} C(x) \right] \quad (19)$$

where $\psi(x)$ is the porosity, D_e is an effective diffusion coefficient, $C(x)$ is the total volume averaged concentration of the component (strontium in our case) and is a scaled version of the liquid/void concentration $C(x) = \psi(x)\bar{c}$. Finally, x is a global slowly varying coordinate. When both porosity and diffusivity are uniform one obtains the standard diffusion equation:

$$\frac{\partial C(x)}{\partial t} = D_e \nabla^2 C(x) \quad (20)$$

D_e decreases with the solid volume fraction $\varnothing = 1 - \psi$, and hence it is smaller than the free diffusion coefficient in the liquid phase.

Assessing the nature of the scaled diffusion coefficient, $\bar{D}_{ap}$, is not immediately trivial. First, the unscaled apparent diffusion coefficient, D_{ap}, appearing in Eq. (1) relates to the concentration of free strontium within the sample and not to the CLF escaping the sample. Indeed, one might claim that under the assumptions of our model, when precipitation is accounted for explicitly; diffusion appears faster when compared with a reactionless case to account for the same value of the CLF. While this may be true for a comparison between D_{ap} and D_e for all cells *within* the cylinder (precipitation reduces the free concentration in every cell, so in order to maintain the same concentration D_e must be smaller than D_{ap}), it lacks the mathematical support for $\bar{D}_{ap}$. Second, $\bar{D}_{ap} = \nu^2 D_{ap}$ and since $\nu < 1$, $\bar{D}_{ap} < D_{ap}$.

Equating Eq. (16) with Eq. (17), to represent equal CLFs at the same time, and denoting $\sqrt{kt} = x$ yields:

$$\sqrt{D_{ap}}\, erf(x) = \sqrt{D_e}\, \frac{2}{\sqrt{\pi}} x \quad (21)$$

Since $erf(x) \leq \frac{2}{\sqrt{\pi}} x$ for all $0 \leq x$ (when $0 < x < 1$, $erf(x)$ and $\frac{2}{\sqrt{\pi}} x$ are practically equal; however, for $1 \leq x$, $\frac{2}{\sqrt{\pi}} x$ can be substantially greater than $erf(x)$ as $erf(x)$ cannot exceed 1), we infer that $D_e < \bar{D}_{ap}$, finally leading to the following inequality:

$$D_e < \bar{D}_{ap} < D_{ap} \quad (22)$$

Two final comments before we proceed with presentation of the results. First, modeling porosity or tortuosity which influence the effective diffusivity is beyond the scope of this work. Second, our work is related to the work by Watson and coworkers (Watson et al., 2010), who combines radial and axial 1D solutions into a single finite cylinder diffusion solution. His work has two additional features: non-isotropic diffusion and nested time kernels for time-dependent diffusion coefficients. Short time expansions for CLFs are derived as well. However, his work does not account for chemical reactions. Accounting for a time-dependent diffusion coefficient is beyond the scope of the current work, and its functional form is not known a-priori.

3. Results

3.1. Leaching experiments

All experimental details were previously described by Bar-Nes et al. (Bar-Nes et al., 2018). Leaching experiments were performed on Portland cement paste samples (CEM I Val d'Azergues, Lafarge, France, w/c = 0.4), spiked with $Sr(NO_3)_2$ (Aldrich chemicals), to a spiked Sr concentration of 3.66 mg Sr/g paste, in addition to an intrinsic Sr concentration of 0.3 mg Sr/g paste.

Two different sets of samples were studied in the present work (the Samples' diameter was approximately 40 mm and their height approximately 15 mm (exact values are substituted in the fitting procedure):

- Samples kept under sealed conditions at room temperature. Nevertheless, these samples were slightly carbonated due to short atmospheric exposure during sample preparation and handling (These samples did not undergo surface polishing, and are denoted here as minor carbonation samples).
- Samples treated for 6 months under 40 °C and atmospheric conditions. For these samples XRD measurements showed a thick carbonation layer of approximately 3500 μm at the outer rim of the samples.

Leaching tests were performed with duplicate samples according to the standard ANSI/ANS-16.1 procedure (ANSI/ANS 16.1, 2017), using deionized water as the leachant solution for 90 days, with leachant replacement at predetermined increased intervals totaling three months.

3.2. Fitting analytical CLF expressions to experimental data of minor carbonation samples

We begin our analysis by fitting the leaching experimental results of two samples that were held at 25 °C in a sealed bag for six months, and hence were only slightly carbonated. Fig. 1 shows fitting of the experimental results in (Method 1313, 2012) with both Eq. (17) (Fig. 1a and c) and Eq. (16) (Fig. 1b and d).

We note that Eq. (17) was fitted in its linear form ($\eta \propto \sqrt{t}$) with zero intercept. Both mathematical expressions are in very good agreement with the experimental data. However, two distinctions should be made when one compares Fig. 1a with Fig. 1b and 1c with Fig. 1d, i.e., besides the fact that a diffusion-kinetic model (with $SrCO_3$ precipitation, Eq. (16)) fits the results slightly better (slightly bigger adjusted R^2) than a diffusion model (without precipitation, Eq. (17)). First, in the diffusion-kinetic model (averaged diffusion-kinetic fitted parameters: $\bar{D}_{ap} = 1.36 \times 10^{-14} m^2/s$ and $k = 8.22 \times 10^{-8} s^{-1}$), all experimental data points either lie on the best fitted curve or very close to it, whereas intermediate data points deviate from the best fitted curve of the standard diffusion model (averaged diffusion coefficient: $\bar{D}_e = 1.01 \times 10^{-14} m^2/s$). Second, the prediction bounds (with 95% confidence level) are narrower for the diffusion-kinetic model, and thus enables one to narrow down prediction ranges for similar strontium release experiments in the future. We believe that this is an important distinction that will be more pronounced for samples with an increasing degree of carbonation and is related to the estimated error of the fitted curve as we now explain.

A small pause for a discussion on the quality of a fit. Comparing R^2 values might be a delicate issue, especially with an underlying non-linear behavior, as indicated in (Shalizi). More information can be gained by comparing the root mean squared error (rmse), which scales the sum of the errors squared by dividing it with the number of degrees of freedom (number of points in the fit minus the number of fitted parameters), and which bares the units of the fitted function (unitless number in our case). For the majority of the points of the leaching curve the rmse is 10–15% from the CLF value in a diffusion only model, whereas the rmse is only 4–7% of this value for a diffusion-kinetic model.

Finally, as was indicated in Section IID, when both diffusion and precipitation are considered, diffusion *appears* somewhat faster when compared with a diffusion only scenario ($\bar{D}_{ap}/D_e = 1.35$).

3.3. Fitting analytical CLF expressions to experimental data of carbonated samples

We continue our analysis by fitting the leaching experimental

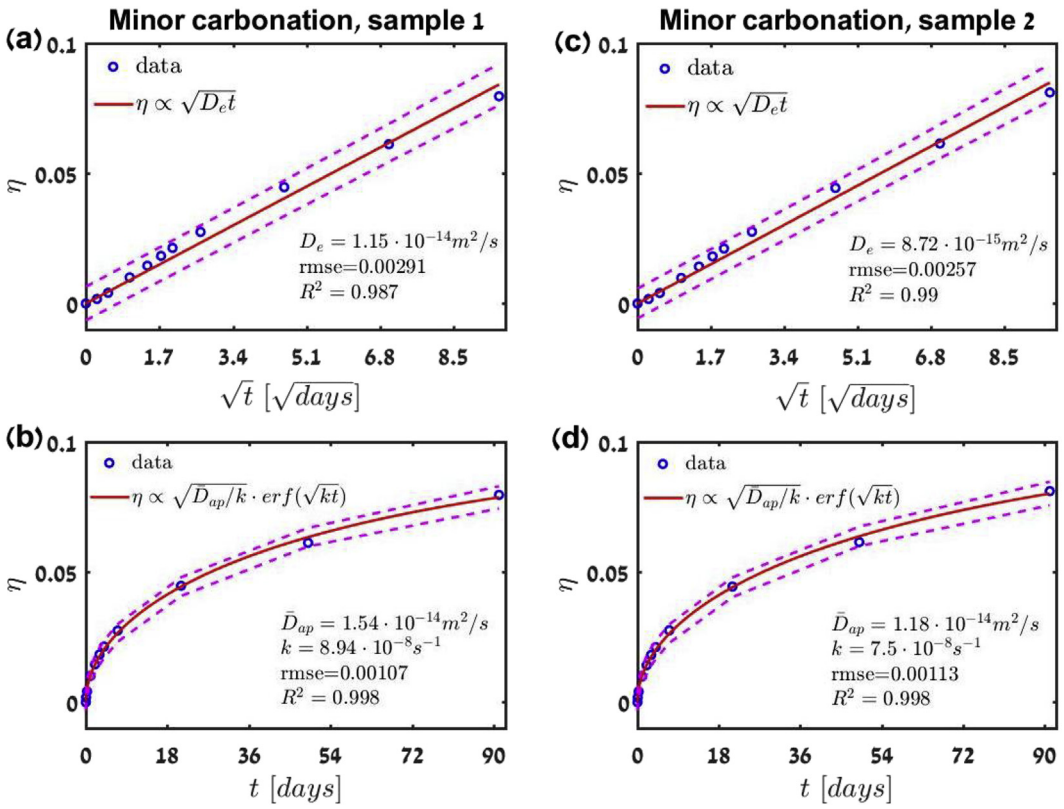

Fig. 1. Cumulative leaching fraction of two minor carbonation samples at 25 °C. Figs (1a) and (1c) represent fitting of the experimental leaching data of two samples when one considers only an effective diffusion mechanism. Figs. (1b) and (1d), respectively, represent fitting of the same data when both diffusion and precipitation are considered simultaneously. Blue hollow circles represent the experimental data in (Bar-Nes et al., 2018), solid red lines represent best fitted curves, and dashed magenta lines represent 95% prediction bounds. (For interpretation of the references to colour in this figure legend, the reader is referred to the Web version of this article.)

results of two samples held at 40 °C, and that were exposed to atmospheric concentration of CO_2 for six months prior to leaching (leaching was carried out at room temperature). Fig. 2 shows fitting of the experimental results in (Bar-Nes et al., 2018) with both Eq. (17) (Fig. 2a and c) and Eq. (16) (Fig. 2b and d).

The features appearing in the set of minor carbonation samples are more pronounced in the major carbonation samples. A diffusion-kinetic model which accounts for both Sr^{2+} diffusion and $SrCO_3$ precipitation is superior to a standard diffusion model. When one compares Fig. 2a with Fig. 2b and 2c with Fig. 2d, two features are clearly visible. First, in the diffusion-kinetic model most experimental data points either fall on the best fitted curve or very close to it (especially at short times), whereas almost all data points (including the ones at short times) deviate from the best fitted curve of the standard diffusion model. Second, the prediction bounds (with 95% confidence level) are narrower for the diffusion-kinetic model. Furthermore, the prediction bounds for the diffusion-kinetic model at short times are quite narrow and expand gradually with time, which further emphasizes the fact that one can narrow down prediction ranges for similar strontium release experiments in the future.

Comparison of the rmse values of the two models shows that it can range between 10 and 40% of the leaching CLF data for a diffusion only model, and between 5 and 20% for the diffusion-kinetic model. This is a dramatic observation, and has consequences on the prediction of leaching behavior and the analysis of standardized leaching tests where precipitation is expected to occur.

The fitted averaged diffusion-kinetic constants for the diffusion-kinetic model are: $\bar{D}_{ap} = 9.51 \times 10^{-15} m^2/s$ and $k = 3.27 \times 10^{-7} s^{-1}$. Once more and as indicated in Section IID, when both diffusion and precipitation are considered, diffusion appears faster when compared with a diffusion only scenario, but more predominantly when compared with the minor carbonation samples ($\bar{D}_{ap}/D_e = 2.3$).

When one compares the minor carbonation samples with the major carbonation samples, one can very intuitively claim that diffusion appears slower and precipitation appears faster for the carbonated samples($\bar{D}_{ap}[major]/\bar{D}_{ap}[minor] \approx 0.7$, $\bar{k}[major]/\bar{k}[minor] \approx 4$). Physically, this might be expected as there is more available carbonate which both increases strontium precipitation (larger excess of carbonate, and hence larger k in pseudo first-order kinetics) which in turn reduces the amount of leachable strontium which is reflected in reduced apparent mobility. However, this is not the full picture, and a very delicate issue as we now explain.

One should not confuse the D_{ap} with $\bar{D}_{ap}$. Indeed, one would expect for major carbonation samples that the *unscaled* apparent diffusion coefficient appearing in Eq. (1) would be substantially greater than the effective diffusion coefficient appearing in Eqs. (17) and (20), as more strontium is expected to precipitate. However, it is *scaled down* by the fraction of leachable strontium prior leaching. This fraction should be smaller when compared with the minor carbonation samples. Therefore, leading to *scaled* apparent diffusion coefficients which are not tremendously different.

3.4. Further analysis of the leaching data: sensitivity analysis and linear graphical analysis

3.4.1. Sensitivity analysis

Our analysis in Sections IIIB and IIIC shows that attaining a certain CLF does not require a dramatic change in the fitted parameters ($\bar{D}_{ap}$ decreases 1.4-fold and k increases 4-fold for the major carbonation samples).

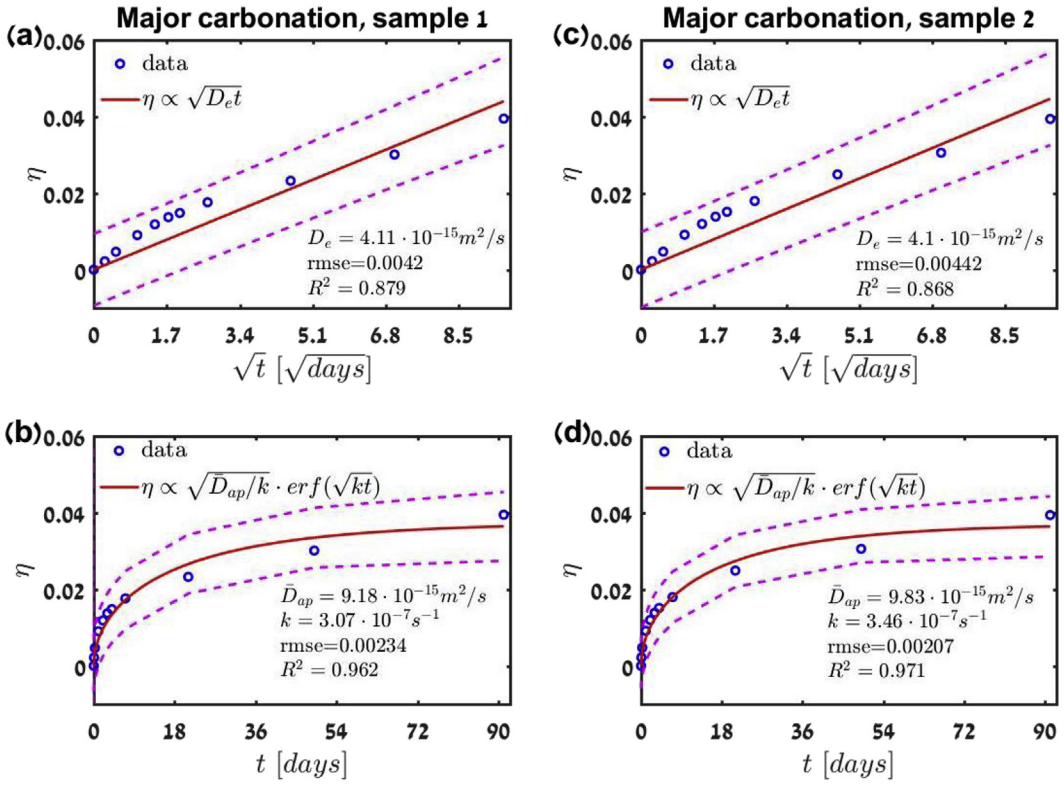

Fig. 2. Cumulative leaching fraction of two carbonated samples at 40 °C. Figs. (2a) and (2c) represent fitting of the experimental leaching data of two samples when one considers only an effective diffusion mechanism. Figs. (2b) and (2d), respectively, represent fitting of the same data when both diffusion and precipitation are considered simultaneously. Blue hollow circles represent the experimental data in (Bar-Nes et al., 2018), solid red lines represent best fitted curves, and dashed magenta lines represent 95% prediction bounds. (For interpretation of the references to colour in this figure legend, the reader is referred to the Web version of this article.)

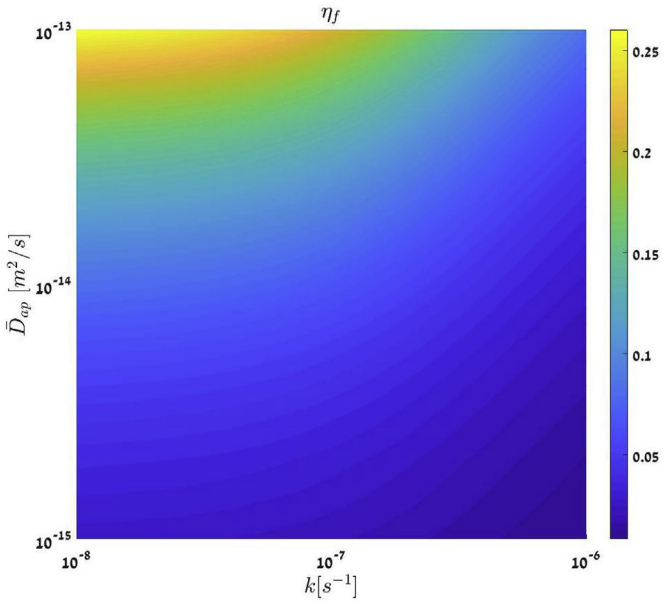

Fig. 3. Final CLF value after 91 days for a standard cylindrical sample as a function of the pseudo first order precipitation rate constant, k, and the scaled apparent diffusion, $\bar{D}_{ap}$.

In order to evaluate a plausible range for the fitted parameters presented in this work, we plot in Fig. 3 the final CLF value after 91 days stemming from the diffusion-kinetic model (Eq. (16)), for a "standard" cylindrical sample of 0.015 m height and 0.015 m radius (quite similar to the samples used for the leaching experiments), as a function of k and $\bar{D}_{ap}$ ranging between $1{\cdot}10^{-8}$-$1{\cdot}10^{-6} s^{-1}$ and $1{\cdot}10^{-15}$-$1{\cdot}10^{-13}\ m^2/s$, respectively, on a logarithmic scale. Inspection of Fig. 3, reveals, that for a final CLF in the range $0.5 \leq \eta_f \leq 0.15$, a wide range of parameters may conspire to yield an identical final CLF value. Therefore, rendering the model not very effective in discriminating between various regimes. However, we wish to make several distinctions here that will help us in elucidating the model's predictive power.

First, for a fixed value of the unscaled apparent diffusion coefficient D_{ap}, appearing in the mass balance equation for free leachable strontium (Eq. (13)), a 4-fold difference in k, leads to a 10-fold difference in leachable strontium after 91 days. Second, when we repeated the diffusion-kinetic fitting procedure ignoring the intrinsic strontium content (leading to a 7.5% decrease in the total strontium content), the precipitation rate constants remain practically unchanged, while the apparent diffusion coefficients showed ~ 1.5-fold and 1.15-fold increase for the minor and major carbonation samples, respectively. Therefore, physically we maintain the same interpretation: in more carbonated environments, one expects faster precipitation rates.

Finally, and most importantly, one has to remember that the fitted CLF parameters are used to predict the leaching curve for the whole-time range of the leaching step. In Fig. 4 we plot the temporal sensitivity of the two diffusion-kinetic parameters. In Fig. 4a we plot the CLF as a function of the scaled apparent diffusion coefficient for three times (91 days, 9 days, and 22 h) and two k values ($5{\cdot}10^{-8} s^{-1}$ and $5{\cdot}10^{-7} s^{-1}$). While for 22 h and 9 days the CLFs are barely distinguishable for a fixed scaled apparent diffusion coefficient very close to the one fitted for both sets of experiments ($\bar{D}_{ap} = 10^{-14} m^2/s$), after 91 days the CLF is doubled for smaller k). In Fig. 4b we plot the CLF as a function of the psuedo first order kinetic rate constant for three times (91 days, 9 days, and 22 h) and two $\bar{D}_{ap}$ values ($5{\cdot}10^{-15}\ m^2/s$ and $5{\cdot}10^{-14}\ m^2/s$). The CLF here is distinguishable for all times for a fixed

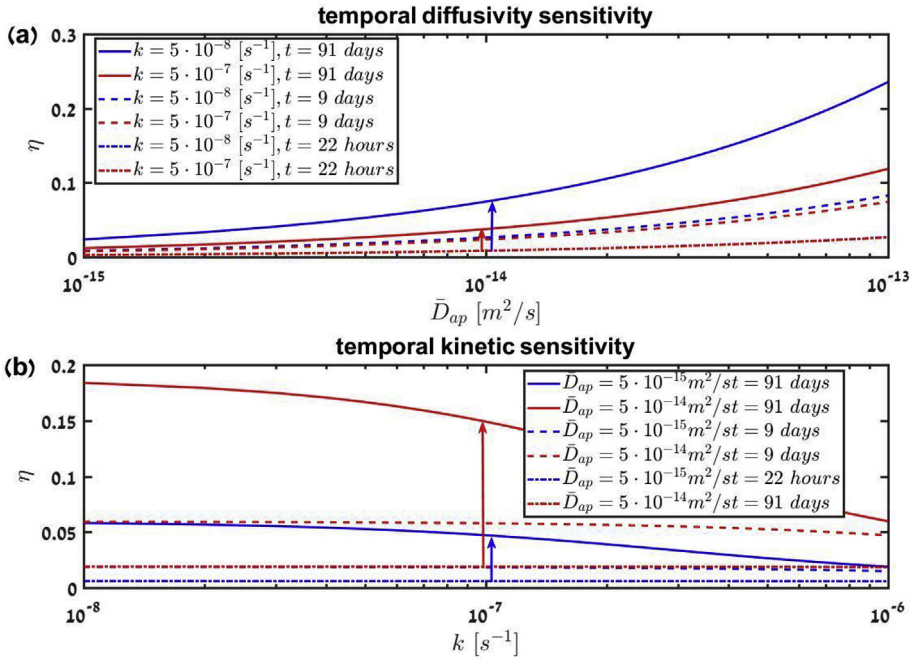

Fig. 4. Temporal sensitivity. Fig. 4a: CLF as a function of the scaled apparent diffusion coefficient for three times (91 days, 9 days, and 22 h) and two k values ($5{\cdot}10^{-8}s^{-1}$ (blue) and $5{\cdot}10^{-7}s^{-1}$ (red)). Fig. 4b: CLF as a function of the pseudo first order kinetic rate constant for three times (91 days, 9 days, and 22 h) and two $\bar{D}_{ap}$ values ($5{\cdot}10^{-15}\,m^2/s$ (blue) and $5{\cdot}10^{-14}\,m^2/s$ (red)).

k = $10^{-7}s^{-1}$, being substantially higher for the larger diffusivity. Therefore, although not perfectly adequate for all cases, we conclude that one can use the CLF derived here for different physical regimes.

3.4.2. Graphical linear analysis

The two fitted models (diffusion vs. diffusion-kinetic) for the minor carbonated samples seem very close, while the two fitted models for the major carbonated samples show substantial differences. In what follows we offer a linear graphical analysis of the two data sets, in a further attempt to elucidate the influential physical phenomena affecting leaching, that may even help us in devising a criterion to prefer the diffusion-kinetic model over the plain diffusion model.

Taking the natural logarithm of Eq. (17) yields:

$$\ln(\eta) = \ln\left(\frac{4\sqrt{D_e}}{\sqrt{\pi}L}\right) + 0.5\ln(t) \tag{23}$$

Therefore, a linear fit of $\ln(\eta)$ vs. $\ln(t)$ should yield a line whose slope is 0.5 and D_e could be extracted from its intercept. In Table 1 below we list the slope and the effective diffusion coefficient for the minor carbonation samples ($R^2 \sim 0.98$, and the rmse was not more than 5% of the $\ln(\eta)$ data):

The ideal slope value of 0.5 falls within the 95% confidence bounds. Therefore, we choose to stick to Eq. (17) as a possible reasonable representation of the minor carbonation leaching data. The downside of this outcome is that no clear distinction can be made ifthe diffusion-kinetic model (Eq. (16)) is superior over a plain diffusion model in describing the minor carbonation leaching data, besides the reduced rmse issue discussed in Section IIIB.

Table 1
Slope (with 95%confidence bounds) and effective diffusion coefficient for a linear fit of $\ln(\eta)$ vs. $\ln(t)$ for minor carbonation samples.

Sample	Slope
Minor 1	0.523 (0.475–0.571)
Minor 2	0.529 (0.482–0.575)

Table 2
Slope (with 95%confidence bounds) and effective diffusion coefficient for a linear fit of $\ln(\eta)$ vs. $\ln(t)$ for major carbonation samples.

Sample	Slope
Major 1	0.38 (0.33–0.43)
Major 2	0.382 (0.333–0.431)

In Table 2 below we list the slope and the effective diffusion coefficient for the major carbonation samples ($R^2 \sim 0.98$, and the rmse was not more than 5% of the $\ln(\eta)$ data):

The ideal slope value of 0.5 falls *outside* the 95% confidence bounds. Combined with the substantial rmse values for the plain square root law, we conclude that Eq. (17) is *not* reasonably representing the major carbonation leaching data.

4. Discussion and conclusion

In this work, we have developed a simple analytical model for strontium leaching from finite cylindrical samples of Portland cement paste. The model accounts for both strontium diffusion (as Sr^{2+}) and precipitation (as $SrCO_3$), and a similar model can be tailored specifically for other simple geometries (i.e. cubic or spherical). The model allows an experimentalist in the field to easily and rapidly fit experimental data with the analytical model, and obtain fitted diffusion-kinetic parameters. The fitted diffusion-kinetic parameters in turn, can be used to estimate the cumulative leaching fraction (CLF) of strontium under similar conditions (of matrix exposure and exposure times) with reasonable confidence bounds.

Extrapolation of CLF values at extended times should be taken with care, as in doing so one assumes that no further changes occur in the immobilizing matrix. However, this is not very realistic as other degradation processes, leading for example to cracking, might develop in the cement matrix, and hence greatly influence the leaching profile. Therefore, extrapolation of CLF's is probably limited to times much shorter than the waste form service life.

The model developed here is global, in the sense that the CLF is derived with homogeneous averaged physical properties. We do acknowledge that in practice the strontium diffusion coefficient and kinetic precipitation rates (and rate constants) are not uniform throughout the sample. Nevertheless, these assumptions enable us to derive simple CLF expressions without ignoring precipitation which is expected in cementitious samples with sufficient carbonate content. Moreover, the rmse stemming from such diffusion-kinetic modeling can be substantially smaller when compared with a plain diffusion model. Therefore, this treatment offers experimentalists conducting leaching tests an easily implementable reliable tool to analyze their data in systems where precipitation is expected to occur. The approach presented here may serve as an alternative to a plain diffusion analysis often found in standardized leaching protocols, and to thermodynamic numerical software.

The CLF's of the minor carbonation samples are in excellent agreement with both a diffusion model and the diffusion-kinetic model, with a slight advantage to the diffusion-kinetic model. Nevertheless, the fact that all experimental data points either lie on the best fitted diffusion-kinetic curve or very close to it with narrower prediction bounds and smaller errors when compared with the standard diffusion model, might indicate that precipitation of strontium carbonate plays a role in the mobility of strontium ions also in samples exposed to minor carbonation.

The fit of a diffusion-kinetic model to the CLF's of the atmospheric carbonation samples is substantially superior over a standard diffusion model. This is a clear indication that precipitation of strontium carbonate cannot be ignored in assessing leaching from cementitious samples with an extensive degree of carbonation.

Furthermore, by introducing a linear graphical analysis we were able to deduce that a plain diffusion model is *not* reasonably representing the major carbonation leaching data, due to a reduced time exponent (0.33) which is far from the well-known time exponent at short diffusion times (0.5), and which cannot be derived from first principles.

One might challenge the “mean-field" approach presented in this work in view of the quality of the fit and other supporting data. As we already indicated the CLFs of the minor carbonation samples are in excellent agreement with the standard diffusion and diffusion-kinetic models. This is an indication that the “mean-field" approach presented in this work is a very suitable approach for application in minor carbonation samples. Indeed, the carbonate concentration in a narrow outer rim of these samples (up to a distance of ~100 μm (Bar-Nes et al., 2018)) resembles that of the bulk. Therefore, a “mean-field" approach in this case gives an adequate representation of an overall averaged matrix.

Although the diffusion-kinetic model is superior over a standard diffusion model when fitted to the CLF's of the atmospheric carbonation samples, the fit is not perfect. This is an indication that the major carbonation samples are less adequately described by an averaged “mean-field" matrix. Indeed, the degree of carbonation in these samples up to a distance of ~3.5 mm from the outer boundaries (Bar-Nes et al., 2018)) is ~6.5-fold when compared with the internal bulk.

Further development of the model, which we intend to pursuit in the future, can be attained with final element software such as COMSOL. In these simulations, one would use a parametric sweep of both the apparent diffusion coefficient and the apparent precipitation rate constant in two concentric, physically different regions: major carbonated outside, and minor carbonated inside. These simulations would be compared with actual leaching data, to determine the kinetic parameters that minimize the difference between experiments and simulations.

Further development of the model discussed here is needed to account for leachable strontium radial and axial distribution and the fraction of precipitated strontium prior to leaching. In addition, the model should be revised for substantial cracking inside the cement matrix, as advection might become the dominant leaching mechanism (and not diffusion).

The drawback of our treatment when compared with freeware and commercial software, such as PHREEQC, HYTEC and LeachXS, is that none of the specific reactions/equilibria are considered; neither in the cement nor between the added component and the cement, when we calculate the CLF. However, one can point to potentially four troubling issues when using the aforementioned programs. First, from the practical point of view, convergence of non-linear partial differential equations coupled with non-linear algebraic equations is not necessarily guaranteed. Second, obtaining a complete thermodynamic and kinetic data set is a hard task, especially in environments in which numerous reactions occur simultaneously. Obtaining such a database is exempted in the treatment presented here. Third, the solution algorithm of the intricate set of equations assumes an identical (and uniform) value for the diffusion coefficients of all constituents. Fourth, thermodynamic software miss out on major constituent concentrations (Ca, Al, Si) for commercial cements which are more complex than simple CSH mixtures with no additives spread over a wide range of pHs and liquid/solid dilution ratios. While the first three issues can be circumvented: in many cases convergence is not an issue (although for some reactive transport simulators, this is still an issue), databases for cements have increased in size in the past decade, and numerical codes are beginning to adopt different diffusion coefficient values for different species; the fourth cannot. How can one completely trust reactive transport codes relying on local equilibrium via LMA or FEM for cements, when they miss out on major constituent concentrations in a variety of equilibrium conditions, which are easier to model when compared with a transport problem? This is further amplified if one wishes to quantify the amount of a possible contaminant, like the strontium discussed here, that shares similar precipitation chemistry with one of the major constituents, calcium in our case. Moreover, in many geochemical codes intricate procedures are implemented to reassess some of the thermodynamic data. That said, we do acknowledge the success of geochemical codes in simulating compositions, especially at steady state/equilibrium over the several decades they exist. Therefore, we do not suggest to abandon numerical reactive transport code, but merely suggest an easily implementable kinetic alternative analytical tool to asses leaching data in systems where precipitation occurs.

Finally, the model presented here is naturally implementable to radioactive decay as it allows for a similar (but not completely identical) kinetic first-order analytical expansion. Furthermore, one can use a similar approach to other radionuclides if a dominant precipitation occurs or tailored to occur in the host matrix, and possibly adopt the model for other modes of degradation combined with carbonation (i.e. radiation).

Appendix A. Derivation of the short time expansion of free Sr in a finite cylinder due to diffusion

Watson et al. (Watson et al., 2010) solve for the fraction of material remaining in a finite cylinder when precipitation does not take place, i.e. the case where$k = 0$, and when perfectly absorbing boundaryconditions are employed together with an initial uniform distribution of diffusing particles. Thus, their solution assumes the form in Eqs. (9) and (10).

A1. Short time expansion of free Sr in the axial coordinate

In order to obtain the short time expansion of $U(t)$ in Eq. (10a), we begin by straightforwardly taking its Laplace transform, $L_{t\to s}[U(t)] \equiv \hat{U}(s)$,

and obtain:

$$\hat{U}(s) = 8\sum_{n=0}^{\infty}\frac{1}{(2n+1)^2\pi^2}\frac{1}{(2n+1)^2\pi^2\frac{D}{H^2}+s} = \frac{1}{s}\left(1 - 8\sum_{n=0}^{\infty}\frac{1}{(2n+1)^2\pi^2+\frac{H^2}{D}s}\right) \tag{A1}$$

Using tabulated identities for the infinite series expansion in Eq. (A1) as a hyperbolic function (Spiegel, 1968) yields:

$$\hat{U}(s) = \frac{1}{s}\left(1 - \frac{2}{\sqrt{\frac{sH^2}{D}}}tanh\left(\frac{1}{2}\sqrt{\frac{sH^2}{D}}\right)\right) \tag{A2}$$

Further expansion of the hyperbolic tangent in Eq. (A2) as an infinite power series yields:

$$\hat{U}(s) = \frac{1}{s}\left(1 - \frac{1}{\sqrt{s}}\frac{2\sqrt{D}}{H}\left(1 + 2\sum_{n=1}^{\infty}(-1)^n e^{-n\frac{H}{\sqrt{D}}\sqrt{s}}\right)\right) \tag{A3}$$

By formally taking the inverse Laplace transform of Eq. (A3) one obtains:

$$U(t) = 1 - \frac{4}{\sqrt{\pi}}\frac{\sqrt{Dt}}{H}\left(1 + \sum_{n=1}^{\infty}\frac{(-1)^n}{\sqrt{t}}\int_0^t dt'\frac{e^{-n^2\frac{H^2}{Dt'}}}{\sqrt{t'}}\right) \tag{A4}$$

Finally, integration by parts of Eq. (*A*4) yields:

$$U(t) = 1 - \frac{4}{\sqrt{\pi}}\frac{\sqrt{Dt}}{H}\left[1 + \sum_{n}(-1)^n\left(2\,e^{-n^2\frac{H^2}{Dt}} - \frac{H}{\sqrt{Dt}}n\sqrt{\pi}\,erfc\left(\frac{n}{2}\frac{H}{\sqrt{Dt}}\right)\right)\right] \tag{A5}$$

The last expression allows us to compute the summation on the right-hand side of Eq. (A5). This summation is plotted versus the dimensionless parameter$\sqrt{Dt/H^2}$, and is denoted as "correction terms". The blue line denotes the value of the summation. The red full circles denote points computed for the parameter values appearing as labels on the horizontal axes.

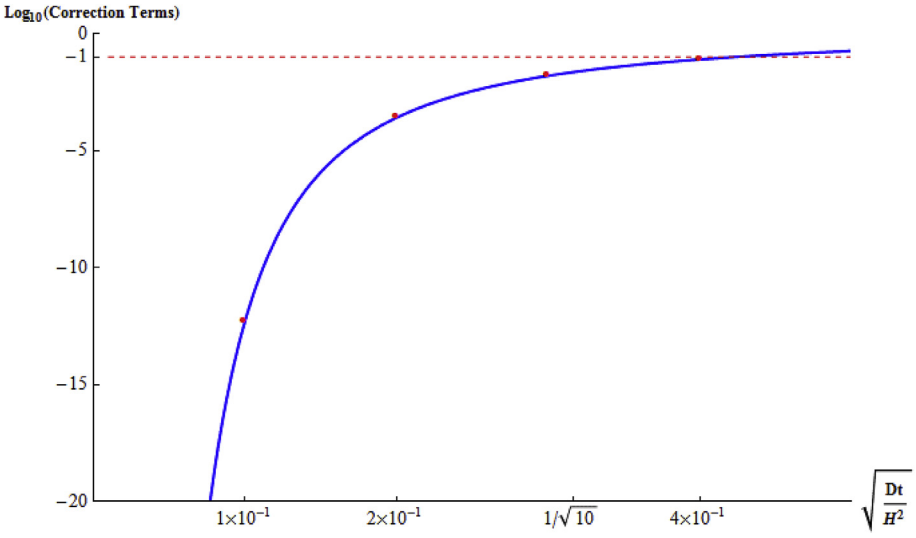

It is quite evident that for sufficiently short times, such that $\sqrt{Dt/H^2} = 0.2$we may safely ignore the summation appearing in Eq. (13) compared to unity and write:

$$U(t) = 1 - \frac{4}{\sqrt{\pi}}\frac{\sqrt{Dt}}{H} \tag{A6}$$

A2. Short time expansion of free Sr in the radial coordinate

In order to obtain the short time expansion of $W(t)$ in Eq. (10a), also here we employ the Laplace transform method. However, the derivation here is a bit more cumbersome. We begin by taking the radial integral of a Laplace transform identity involving Bessel functions (Watson, 1995):

$$L_{t\to s}\int_{r=0}^{R} rdr\left[1 - 2\sum_{n=1}^{\infty}e^{-\lambda_n^2 t/R^2}\frac{J_0(\lambda_n r/R)}{\lambda_n J_1(\lambda_n)}\right] = \int_{r=0}^{R} rdr\frac{I_1(r\sqrt{s})}{sI_0(R\sqrt{s})} \tag{A7}$$

Performing the integrals on both sides of Eq. (A8) with an appropriate change of variables, together with the linearity of Laplace transforms, yields after some algebra:

$$L_{t\to s}\left[4\sum_{n=1}^{\infty}\frac{1}{\lambda_n^2}e^{-\lambda_n^2 t/R^2}\right]=\frac{1}{s}-\frac{2}{Rs\sqrt{s}}\frac{I_1(R\sqrt{s})}{I_0(R\sqrt{s})} \tag{A8}$$

By making a change of variable $t \to Dt$, and using a Laplace transform identity involving scaled variables (Spiegel, 1968), we finally arrive at:

$$L_{t\to s}\left[4\sum_{n=1}^{\infty}\frac{1}{\lambda_n^2}e^{-\lambda_n^2 t/R^2}\right]=L_{t\to s}[W(t)]\equiv\hat{W}(s)=\frac{1}{s}\left[1-\frac{2}{R\sqrt{s/D}}\frac{I_1(R\sqrt{s/D})}{I_0(R\sqrt{s/D})}\right] \tag{A9}$$

We now seek to find a short time expansion for free Sr in the radial coordinate. We begin by noting that for practical purposes in the vicinity of $t \to 0$, the radial function, $W(t)$, can be approximated by:

$$L_{s\to t}[\hat{W}(s\to\infty)]\approx W(t\to 0) \tag{A10}$$

We note that we use equation (A10) for the leaching function itself and not for its limiting value, for which we can use the initial value theorem: $L_{s\to t}[s\hat{W}(s\to\infty)]=W(t\to 0)$. By using an approximation for the ratio of modified Bessel functions when $s \to \infty$ (Karpov et al., 2001), we may write:

$$\hat{W}(s)\approx\frac{1}{s}\left[1-\frac{2}{R\sqrt{s/D}}\left(1-\frac{1}{2R\sqrt{s/D}}-\frac{1}{8R^2s/D}+\cdots\right)\right] \tag{A11}$$

Taking the inverse Laplace transform of Eq. (A11) yields $W(t)$ when $t \to 0$:

$$W(t)\approx 1-\frac{4}{\sqrt{\pi}}\frac{\sqrt{Dt}}{R}+\frac{Dt}{R^2}+\frac{1}{3\sqrt{\pi}}\frac{\sqrt{(Dt)^3}}{R^3}-\cdots \tag{A12}$$

When all pre-factors are included properly, even for values of $\sqrt{Dt}/R$ as high as 0.05, the second, third, and fourth terms are numerically equal to $1.1E^{-1}$, $2.5E^{-3}$, *and* $2.4E^{-5}$, respectively. Therefore, for $\sqrt{Dt}/R < 0.05$ values we can safely write:

$$W(t)=1-\frac{4}{\sqrt{\pi}}\frac{\sqrt{Dt}}{R} \tag{A13}$$

Indeed, we note that in all the curve fitting procedures we carried out in this work, we never exceeded a value of $\sqrt{Dt}/R = 0.02$. Combining Eqs. (A6) and (A13), and leaving only a square root dependence on time, we finally arrive at Eq. (11) for free Sr^{2+}.

References

Abdel Rahman, R.O., Zaki, A.A., 2011. Comparative study conceptual models: Cs leaching from different ILW cement-based materials. Chem. Eng. J. 173, 722–736.

ANSI/ANS 16.1, "Measurement of the Leachability of Solidified Low-level Radioactive Wastes by a Short-term Test Procedure (R2017)".

Bar-Nes, G., Klein-Ben David, O., Chomat, L., Macé, N., Arbel-Haddad, M., Poyet, S., 2018. Sr immobilization in irradiated Portland cement paste exposed to carbonation. Cement Concr. Res. 107, 152–162.

Brinkley, S.R., 1946. Note on the conditions for equilibrium for systems with many components. J. Chem. Phys. 14, 563–564.

Brinkley, S.R., 1947. Calculation of the equilibrium composition of systems of many constituents. J. Chem. Phys. 15, 107–110.

Bruna, M., Chapman, S.J., 2015. Diffusion in spatially varying porous media. SIAM J. Appl. Math. 75, 1648–1674.

CEN/TS 14405, Comité Européen de Normalisation (2004).

CEN/TS 14429, Comité Européen de Normalisation (2005).

CEN/TS 15863, Comité Européen de Normalisation (2009).

Crank, J., 1975. The Mathematics of Diffusion, second ed. Clarendon Press, Oxford.

Dikin, I.I., 1967. Iterative solution of problems of linear and quadratic programming. Dokl. Akad. Nauk SSSR 174, 747–748.

Karpov, I.K., Chudnenko, K.V., Kulik, D.A., 1997. Modeling chemical mass transfer in geochemical processes: thermodynamic relations, conditions of equilibria, and numerical algorithms. Am. J. Sci. 277, 767–806.

Karpov, I.K., Chudnenko, K.V., Kulik, D.A., Avchenko, O.V., Bychinskii, V.A., 2001. Minimization of Gibbs free energy in geochemical systems by convex programming. Geochem. Int. 39, 1207–1219.

Kosson, D.S., van der Sloot, H.A., Stefanski, L., Baldwin, M., 2014. Leaching Test Relationships, Laboratory-to-Field Comparisons and Recommendations for Leaching Evaluation using the Leaching Environmental Assessment Framework (LEAF). EPA 600/R-14 061.

Kulik, D.A., Wagner, T., Dmytrieva, S.V., Kosakowski, G., Hingerl, F.F., Chudnenko, K.V., Berner, U., 2013. GEM-Selektor geochemical modeling package: revised algorithm and GEMS3K numerical kernel for coupled simulation codes. Comput. Geosci. 17, 1–24.

Method 1313, US EPA (2012).

Method 1314, US EPA (2013).

Method 1315, 2013. US EPA.

Morel, F., Morgan, J., 1972. A numerical method for computing equilibria in aqueous chemical systems. Environ. Sci. Technol. 6, 58–67.

Parkhurst, D.L., 1995. User's Guide to PHREEQC. USGS investigation report 95-4227.

Rubin, J., 1983. Transport of reacting solutes in porous media: relation between mathematical nature of problem formulation and chemical nature of reactions. Water Resour. Res. 19, 1231–1252.

Seigneur, N., L'hopital, E., Dauzeres, A., Voutilainen, M., Detilleux, V., Labeau, P.E., Dubus, A., 2017. Numerical representative elementary volume generation of a simplified cement paste and estimation of its diffusivity and comparison with dedicated experiments. J. Porous Media 20 (1), 29–46.

Shalizi C., "Modern Regression", lecture 10, Carnegie Mellon University, Pittsburg, Pennsylvania, USA.

Soler, J.M., 2007. Thermodynamic Description of the Solubility of CSH Gels in Hydrated Portland Cement. Posiva OY Working report 2007-2088.

Spiegel, M.R., 1968. Mathematical Handbook of Formulas and Tables", Schaum's Outline Series. McGraw-Hill books.

Ukrainczyk, N., Koenders, A.B., 2014. Representative elementary volumes for 3D modeling of mass transport in cementitious materials. Model. Simulat. Mater. Sci. Eng. 22 (3) 035001.

Valdés-Prada, F.J., Ramírez, J.A., 2011. A volume averaging approach for asymmetric diffusion in porous media. J. Chem. Phys. 134, 204709.

Watson, G.N., 1995. A Treatise on the Theory of Bessel Functions, second ed. Cambridge University Press.

Watson, E.B., Wanser, K.H., Farley, K.A., 2010. Anisotropic diffusion in a finite cylinder, with geochemical applications. Geochem. Cosmochim. Acta 74, 614–633.

White, W.B., Johnson, S.M., Dantzig, G.B., 1957. Chemical equilibrium in complex mixtures. The RAND Corporation 1059.